The Effect of Surface Topography and Surface Albedo Variation on the Radiation Environment of Palmer Station, Antarctic

P. Ricchiazzi and C. Gautier
Institute for Computational Earth System Science
University of California, Santa Barbara
Santa Barbara, California

Abstract

We present results from a 3-D radiative transfer simulation of the radiation environment of Palmer Station, Antarctica. The model results for several wavelength bands in the SW indicate that plane-parallel models of either top of the atmosphere (TOA) radiance or surface irradiance may produce significant errors when applied to regions of high surface albedo heterogeneity.

Introduction

Remote sensing of high-latitude regions requires consideration of a number of challenging issues not usually incorporated in standard radiation models. In addition to the well-known problems of discriminating between clouds and high albedo surfaces, low sun angles make satellite observations of the surface difficult to interpret. Another set of problems emerges in the analysis of the surface radiation measurements. The increased surface coverage of snow and ice increases multiple reflection and causes a significant sensitivity of downwelling irradiance on the surface reflectivity. The much greater importance of the surface makes it important to consider how surface topography and albedo inhomogeneity affect the radiation field. These geometrical effects must be understood in order to make quantitative use of the satellite and surface radiation measurements.

We have undertaken a thorough study of the radiation environment at Palmer Station, Antarctica (Lubin et al. 1994; Ricchiazzi et al. 1995) in hopes of developing insight into how surface radiation levels of UVB, UVA, and visible radiation can be derived from satellite imagery. Here we present results from a simulation of the 3-D radiation environment of the station. The analysis was performed with a new Monte Carlo radiative transfer (RT) code, SAMCRT, that includes explicitly the interaction of radiation with heterogeneous surface features.

Radiative Transfer Model

The SAMCRT code treats surface-radiation processes in fine detail, at the expense of somewhat simplified atmospheric treatment, at least as compared with state-of-the-art atmospheric Monte Carlo RT models. The main physical mechanisms treated by SAMCRT are described below.

Since high-latitude clouds tend to show little vertical development, we assume clouds are plane-parallel and of negligible thickness. The scattering properties of the cloud "scattering-plane" are based on discrete ordinate radiative transfer (DISORT) (Stamnes et al. 1988) calculations for a range of cloud optical depths and incident photon zenith angles. The angular probability distributions for the zenith and azimuth angles of cloud-scattered photons are derived from considering the reflected and transmitted radiance just above and below the cloud layer. Clouds are assumed to consist of spherical water droplets of effective radius 10 μ. No horizontal transport is allowed within the cloud.

Similarly, photon interactions with a snow surface are derived from DISORT calculations for a infinitely thick snow pack consisting of spherical ice grains with an effective radius of 100 μ. The surface layer is segmented into facets that conform to topographics features. The ocean surface is modeled as a Lambertian reflector with a wavelength-dependent albedo.

The distribution of gaseous absorbers is assumed to vary exponentially in the vertical direction with different scale heights for mixed gases and water vapor. For the calculations presented here, the total precipitable water and water vapor scale height is set at 0.2 g/cm^2 and 3.0 km, respectively. The ozone density distribution has two values, with 25 DU in the troposphere (z < 15 km) and 300 DU in the stratosphere (15 < z < 30 km). Absorption by gases is based on fits to

LOWTRAN 7 transmission functions and is carried forward through successive scatterings as a photon "de-weighting" factor.

Atmospheric scattering outside of the cloud layer (e.g., due to Rayleigh scattering or aerosols) is allowed to occur anywhere within the computational volume, from 0 to 100 km altitude.

The surface model includes topographic information of the southwest corner of Anvers Island, over a 20-km x 20-km square centered on Palmer Station. The surface grid is made up of 10,000 facets, each of which is 200 meters on a side. We use 10^8 photons per run. So 10,000 photons are potentially available to sample each surface element.

Since photon trajectories obey cyclic boundary conditions, surface features within the model have a spurious 20-km periodicity. The radiation environment of Palmer Station will be adequately simulated if the influence of surface elements further than 10 km have a small impact on local conditions. In any case, grid points near the boundary will be subject to unrealistic influence from surface elements from the opposite boundary.

Results

We have used SAMCRT to model-nm wide spectral bands at 300 nm and 410 nm and relatively broad bands that duplicate the filter functions of National Oceanic and Atmospheric Administration's (NOAA) advanced very high resolution radiometer (AVHRR) channels 1 and 2.

Figure 1 shows simulated top of the atmosphere (TOA) radiance in AVHRR channel 1 for photons having a propagation direction within 30 degrees of zenith. The top panel shows results for clear conditions and the lower for cloud optical depth of 5. For both calculations, the solar zenith and azimuth angles are set at 59.25 and 53.0 degrees, respectively (the solar coordinates for 9 a.m, October 31). North is toward the top of the image.

Though the surface relief is not very large for this part of the island, the clear sky simulation shows a definite reduction of radiance for regions sloping downward in the southwest direction, away from the direction of illumination. This result provides a quantitative measure of the topographic effect that could be expected from satellite-based estimates of surface albedo.

The lower panel of Figure 1 shows radiance computed for overcast conditions, for cloud optical depth 5 and cloud

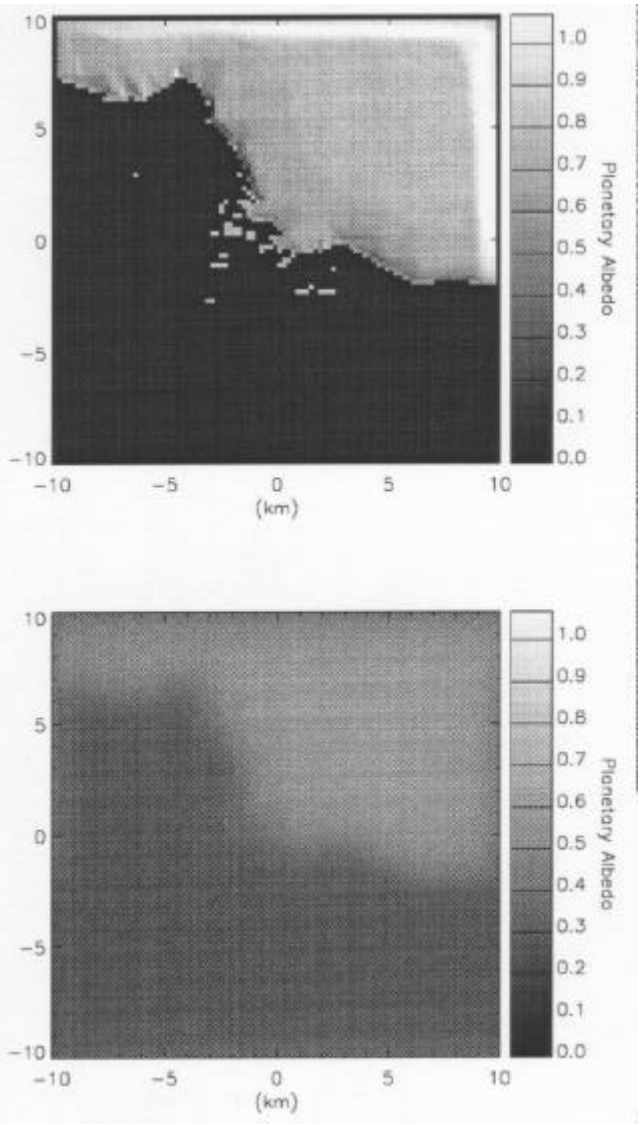

Figure 1. Simulated TOA radiance in AVHRR channel 1 for clear sky conditions (top) and for cloud optical depth 10 (bottom).

height 1 km. In this case, the island outlines are still visible, but any topographic effect is hard to detect. The blurring along the coast line has a gradient length set by cloud height. When we repeated this calculation for a cloud height of 5 km, blurring was greatly increased. Evidently, when such high albedo contracts are present, the blurring of the underlying surface must be taken into account in International Satellite Cloud Climatology Project (ISCCP) style satellite retrievals of cloud optical depth, particularly when high clouds are present.

The surface irradiance predicted for a cloud optical depth 20 is shown in Figure 2. In this calculation, the cloud height is fixed at 1 km and solar coordinates are the same as in Figure 1. We have performed similar calculations for a wide range of cloud optical depths and have noted that the reduction in irradiance with increased optical depth is slower over island than over ocean. This is consistent with plane-parallel results and conforms to the notion that multiple reflection can nearly cancel the cloud attenuation when the surface albedo is very high. However, the interesting aspect of these results is the fairly large distance from the coast over which the island surface irradiance is reduced by the proximity of a low albedo surface. In fact, even towards the center of the island, the surface irradiance does not quite attain the value expected from an infinite plane-parallel snow surface.

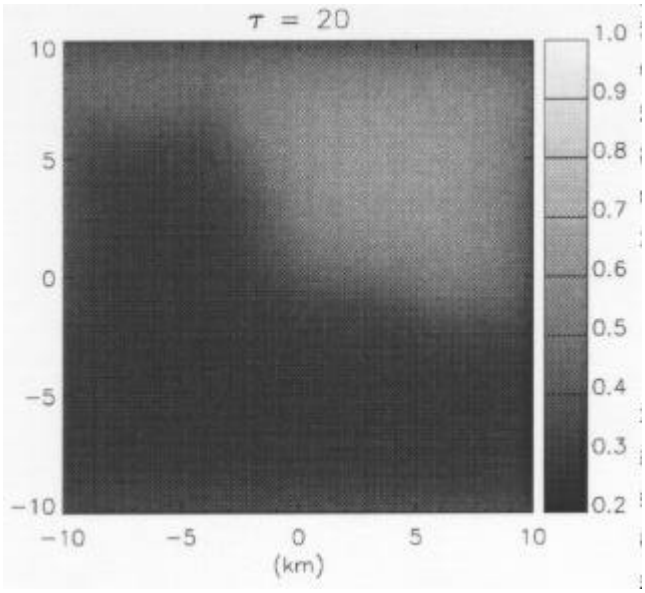

Figure 2. AVHRR-1 surface irradiance under a cloud of optical depth 20 and cloud height of 1 km.

To investigate this issue further, we show in Figure 3 transects of the surface irradiance in four spectral bands, AVHRR-1, AVHRR-2, 410 nm and 300 nm. In these plots, the transect over the SAMCRT surface grid is indicated with a solid line. The transect path runs diagonally from the southwest to northeast corner of the surface grid and each line is labeled on the right with the cloud optical depth used in the calculation. For comparison, we also show results from SBDART (Ricchiazzi et al. 1995), a detailed plane-parallel RT code. The SBDART results for 0%, 50%, and 100% surface snow fraction are indicated by the box, triangle, and diamond symbols, respectively. Presumably, since Palmer Station is on the coast, the conditions at the station should be

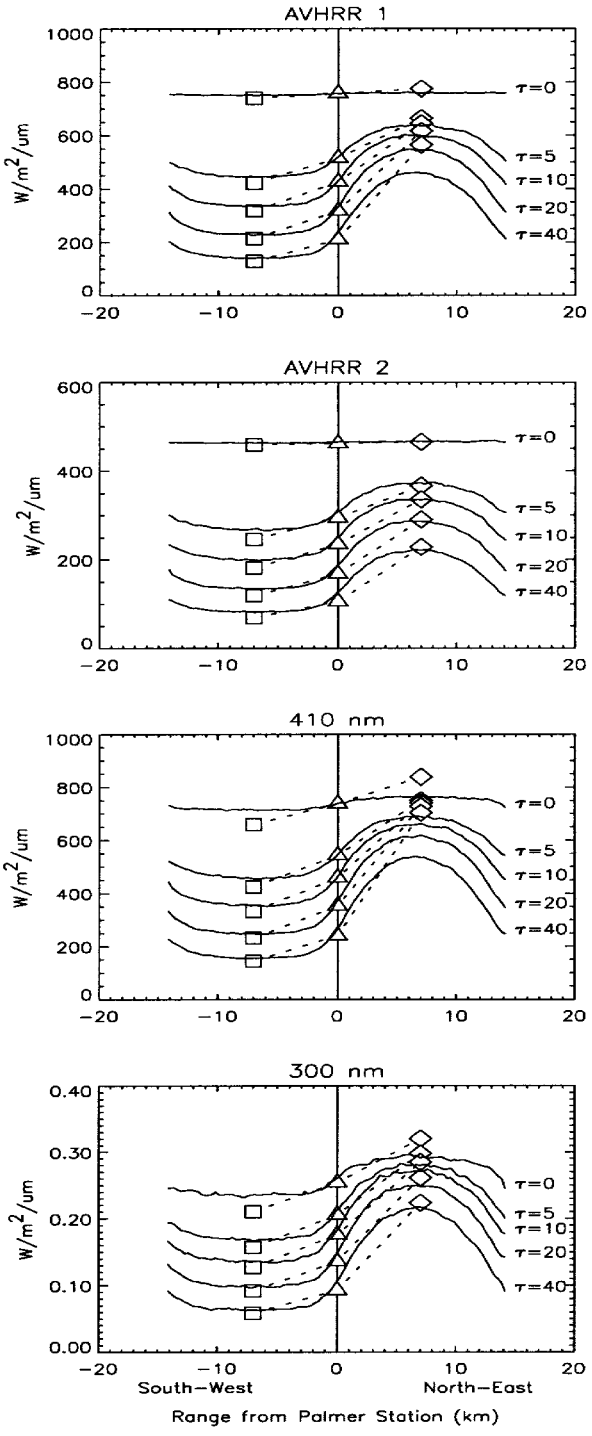

Figure 3. Surface irradiance transects for AVHRR-1, AVHRR-2, 410 nm, and 300 nm. Transect runs from southwest to northeast corners of the surface grid. Results for a homogeneous surface of 0%, 50% and 100% snow are indicated by square, triangle, and diamond symbols, respectively.

well represented by SBDART's 50% snow prediction. And if horizontal dimensions of the surface and grid are sufficiently large, effects of the snow/ocean albedo contrast should be negligible at either the center of the ocean or island, that is, at ±7 km along the transect line. If this is the case, the SAMCRT results at ±7 km should match up with SBDART predictions for 0% and 100% snow fraction.

Consider first the AVHRR channels. In the clear sky case ($\tau = 0$) the SAMCRT transects show very little dependence on surface condition and agree quite well with the SBDART results. As the cloud optical depth is increased, however, SAMCRT's AVHRR-1 results at +7 km are significantly less than the SBDART predictions for 100% snow. These differences are not due to modeling inaccuracies. When SAMCRT is applied to a homogeneous Lambertian surface, the results show better than 3% agreement with the SBDART results for a wide range of cloud optical depth and surface albedo. We have also run SAMCRT with the surface grid artificially enlarged in horizontal dimension by a factor of 5, but otherwise the same as the grid used in the runs shown in Figure 3. These runs indicate that the AVHRR-1 irradiance predicted by SAMCRT does indeed attain the level predicted by SBDART, but only when the distance from the nearest coast exceeds about 10 km.

The predictions for AVHRR-2 are interesting since they seem to agree well with SBDART for all cloud optical depths. At the longer wavelengths received by this channel, the reflectivity of snow is significantly smaller while the absorption by water vapor and oxygen is larger, compared with AVHRR-1. Both factors decrease the importance of multiple reflection and cause a decrease in the influence of distant surface elements.

A similar line of reasoning explains the behavior of the 410-nm and 300-nm channels. In these spectral bands, the snow albedo is very high and nearly the same for both channels. While there is no atmospheric absorption in the 410-nm band, the 300-nm band is subject to strong ozone absorption. Attenuation by stratospheric ozone does not directly impact the non-local surface effect in the 300-nm band because it does not directly influence the transport of radiation below the cloud. Compared with the stratospheric component, tropospheric absorption is relatively small. However, it can become significant when amplified by multiple reflection between surface and cloud and can lead to a reduced influence of distant surface elements. This effect is evident in the SAMCRT results, which show very large deviations from SBDART's 100% snow predictions for the 410-nm band and small deviations for 300 nm, especially for large cloud optical depth. For small cloud optical depth, both the 300-nm and 410-nm bands show more non-local effect than AVHRR-1. This is due to an increased importance of Rayleigh scattering, which has a mean scattering altitude somewhat greater than that of low clouds.

Conclusions

We have undertaken a study of the radiation environment of Palmer Station using a 3-D radiative transfer model that explicitly includes radiative interactions with heterogeneous surface features. The main results of our analysis are

- In overcast conditions, increasing the cloud base height from 1 to 5 km greatly increases the influence of distant surface elements on the local downwelling irradiance. The effect of increased cloud height on the TOA radiance is to blur the transition from cloud-over-ocean to cloud-over-snow regions.

- Even at a cloud base height of 1 km, the surface albedo's radius of influence is surprisingly large, especially for spectral bands with low atmospheric absorption (i.e., 410 nm or AVHRR-1). For these spectral bands, the center of the "island" feels the influence of the dark ocean, though more than 7 km from the coast. However, the radius of influence is smaller when considering ocean areas. The off-shore surface irradiance approaches 100% ocean values within 3 or 4 km of the coast.

- The surface irradiance in spectral bands with high atmospheric absorption or lower snow reflectance (i.e., 300 nm or AVHRR-2) is less sensitive to the reflectivity of distant surface elements.

Though these results are based on ice-free ocean conditions, they provide a basis on which to estimate effects for other sea ice distributions.

Acknowledgments

This work was supported in part by the Atmospheric Radiation Measurement Program of the U.S. Department of Energy under grant 90ER61062, and in part by the National Science Foundation under grant OPP9317120.

References

Lubin, D., P. Ricchiazzi, C. Gautier, and R. H. Whritner, 1994: A method for mapping Antarctic surface UV radiation using multispectral satellite imagery. *Ultraviolet Radiation in Antarctica: Measurement and Biologic Effects*, C. W. Weiler and P. A. Penhale, eds. American Geophysical Union Antarctic Research Series, American Geophysical Union, Washington, D.C.

Ricchiazzi, P. J., C. Gautier, and D. Lubin, 1995: Cloud scattering optical depth and local surface albedo in the Antarctic: Simultaneous retrieval using ground-based radiometry. *J. Geophy. Res*., **100**, 21091-21104.

Stamnes, K., S.-C. Tsay, W. J. Wiscombe, and K. Jayaweera, 1988: Numerically stable algorithm for discrete-ordinate-method radiative transfer in multiple scattering and emitting layered media. *Appl. Opt*., **27**, 2502-2509.